Author's Accepted Manuscript

Soft tissue displacement over pelvic anatomical
landmarks during 3-D hip movements

V. Camomilla, T. Bonci, A. Cappozzo

This is a PDF file of an unedited manuscript that has been accepted for
publication. As a service to our customers we are providing this early version of
the manuscript. The manuscript will undergo copyediting, typesetting, and
review of the resulting galley proof before it is published in its final citable form.
Please note that during the production process errors may be discovered which
could affect the content, and all legal disclaimers that apply to the journal pertain.

Soft tissue displacement over pelvic anatomical landmarks during 3-D hip movements

V. Camomilla[a,b], T. Bonci[b,c], A. Cappozzo[a,b]

[a]Department of Movement, Human and Health Sciences, Università degli Studi di Roma ''Foro Italico'', Rome, Italy

[b]Interuniversity Centre of Bioengineering of the Human Neuromusculoskeletal System, Università degli Studi di Roma "Foro Italico", Rome, Italy

[c]Life and Health Sciences, Aston University, Birmingham, United Kingdom

[*]Corresponding author at: University of Rome "Foro Italico", piazza Lauro De Bosis 15, 00135 Rome − Italy. Tel.: +0039 06 36733522; fax: +0039 06 36733517. valentina.camomilla@uniroma4.it

Abstract

The position, in a pelvis-embedded anatomical coordinate system, of skin points located over the following anatomical landmarks (AL) was determined while the hip assumed different spatial postures: right and left anterior-superior and posterior-superior iliac spines, and the sacrum. Postures were selected as occurring during walking and during a flexion-extension and circumduction movement, as used to determine the hip joint centre position (star-arc movement). Five volunteers, characterized by a wide range of body mass indices (22-37), were investigated. Subject-specific MRI pelvis digital bone models were obtained. For each posture, the pose of the pelvis-embedded anatomical coordinate system was determined by registering this bone model with points digitized over bony prominences of the pelvis, using a wand carrying a marker-cluster and stereophotogrammetry. The knowledge of how the position of the skin points varies as a function of the hip posture provided information regarding the soft tissue artefact (STA) that would affect skin markers located over those points during stereophotogrammetric movement analysis. The STA was described in terms of amplitude (relative to the position of the AL during an orthostatic posture), pelvis orientation and diameter (distance between the positions of the AL which were farthest away from each other). The STA amplitude, exhibited, over all postures, a median [inter-quartile] value of 9[6] and 16[11] mm, for normal and overweight volunteers, respectively. Consequent errors in pelvic pose were in the range 1-9 and 4-11 degrees, for the two groups respectively. STA

diameters were larger for the star-arc than for the walking postures, and the direction was predominantly upwards.

Keywords

Soft tissue artefact; Human movement analysis; Stereophotogrammetry; Pelvis; Multiple anatomical calibration

1. Introduction

The movement between markers attached to the skin surface, as used in stereophotogrammetry for the analysis of human motion, and the underlying bone (soft tissue artefact: STA) has been investigated in various body segments and during different motor tasks. This was made possible by simultaneously monitoring the movement of the skin markers and of the underlying bone using methods such as intracortical pins (Andersen et al., 2012; Andriacchi et al., 1998; Benoit et al., 2006; Camomilla et al., 2013; Cappozzo et al., 1996; Cereatti et al., 2009; Dal Maso et al., 2016; Fuller et al., 1997; Lafortune et al., 1992; Ramsey et al., 2003; Reinschmidt et al., 1997; Westblad et al., 2000), percutaneous bone tracking devices (Houck et al., 2004; Holden et al., 1997; Manal et al., 2000), fluoroscopy (Akbarshahi et al., 2010; Charbonnier et al., 2014; Kuo et al., 2011; Sati et al., 1996; Stagni et al., 2005; Tsai et al., 2009, 2011), or X-rays (Maslen and Ackland, 1994).

Although a reasonable amount of relevant information concerning the lower and upper limb segments is available in the literature (Leardini et al., 2005; Peters et al., 2010), only two studies provided information on the STA that affects the pelvis. One investigation was performed during gait and sit to stand using markers mounted on pins inserted into the sacrum (Rozumalski et al., 2008). This study showed larger STA for the anterior-superior than for the posterior iliac spine areas, and in the craniocaudal direction. A non-invasive assessment of pelvic STA was performed relying on the estimate of the pelvic bone-pose provided by a multiple anatomical calibration (Hara et al., 2014). This technique involves static calibrations performed through manual palpation of relevant anatomical landmarks (ALs) and consequent identification of their position using stereophotogrammetry through the range of motion of the joint of interest (Cappello et al., 1997). In this way, the STA issue is bypassed and a reliable pelvis pose can be assessed in each posture of interest. This method, besides not showing the STA components caused by the wobbling of the soft tissues, suffers from unavoidable intra-operator variability in the multiple identification of the ALs. This

variability has been found to have a root mean square (rms) value in the range 11-20 mm causing pelvic orientation rms variability between 2 and 4 deg (Della Croce et al., 1999). Moreover, the hip postures investigated in Hara et al. (2014) simulated movements occurring only in the sagittal plane, which is not the case in locomotion and other functional motor tasks. A special case in which the STA affecting the pelvis is generated during a hip 3-D movement, characterized by large flexion-extensions and adduction-abductions excursions (the so-named star-arc movement; Camomilla et al., 2006), is the estimate of the hip joint centre position using a functional approach. The STA affecting this estimate (Kainz et al., 2015) heavily impacts the accuracy of movement analysis (Stagni et al., 2000). This calls for an accurate characterization of the artefact (Camomilla et al., 2013) as a premise for its compensation (De Rosario et al., 2013; Rouhandeh et al., 2014a). Another limitation of the study of Hara et al. (2014) is that only information relative to normal-weight subjects is provided.

Therefore, the aim of this study was to assess pelvic STA expanding current available knowledge to 3-D hip poses, including those normally occurring during walking and during the above-mentioned star–arc movement, and to volunteers characterized by a wide range of body mass indices (BMIs). An experimental approach similar to that illustrated in Hara et al. (2014) was used, but with an enhanced anatomical calibration technique, named UP-CAST and illustrated in Donati et al. (2007, 2008), which drastically reduces the intra-operator variability of pelvic orientation estimation.

2. Materials and Methods

Five healthy volunteers with body mass index ranging from 22 to 37 (Table 1) participated in the study after signing a written informed consent.

2.1. Subject–specific digital bone models

In this study, the digital model of the pelvis of each volunteer was acquired experimentally using MRI. The acquisitions were performed with a 1.5T whole-body scanner (Master Philips Medical System, Best, The Netherlands). Each volunteer laid supine in the body MRI coil and underwent one MRI axial scan. The scanning ranged from the iliac crests to the ischial tuberosities of the pelvis skeleton. The bone–specific imaging protocol included series of T1–weighted spin echo images, with a repetition time of 10.0 ms and an echo time of 4.6 ms. The images had an in–plane resolution of 1.8 mm (sectional image 256x256 pixel,

field of view of 450 mm) and an in–between plane resolution of 2.5 mm. The bone digital models were thereafter reconstructed (AMIRA®, version 5.5, default settings, Stalling et al., 2005).

Four ALs were virtually palpated on the bone models using the written and pictorial instructions delivered in the Vakhum EU project (Van Sint Jan, 2007): right and left anterior superior iliac spines (RASIS, LASIS), right and left posterior superior iliac spines (RPSIS, LPSIS). These ALs were used to associate to each bone model an anatomical coordinate system (ACS, Fig. 1) defined as in Cappozzo et al., (1995).

On the bone model surface, points covered with a layer of soft tissue that allows for their palpation through the skin, hereafter called model unlabelled–points (mUPs), were also identified for the sake of the registration exercise illustrated in the following section (black points in Fig. 1). Right and left hip joint centre positions were identified (RHJC and LHJC) as the centre of the spheres that fitted points selected in the acetabula areas using the sphere fitting algorithm implemented in Rapid Form (version 5.7, Inus Technology, Seoul, South Korea). The bone digital model, the mUPs, ALs, and the HJCs were represented in the pelvic ACS and used to perform the anatomical calibration procedure based on the UP–CAST method (Donati et al., 2007) as detailed in Section 2.1.

2.2. Stereophotogrammetric experimental protocol

The following anatomical landmarks were manually palpated and marked with a felt pen on the skin of each volunteer while he/she was standing in orthostatic posture (^{s}ALs, denoted with the left superscript s): the iliac spines (^{s}RASIS, ^{s}LASIS, ^{s}RPSIS, ^{s}LPSIS), the sacrum (^{s}SACR), and the femur lateral and medial epicondyles (^{s}RLE, ^{s}RME) of the right leg.

The volunteers were then equipped with seven skin–markers glued on the pelvis (P1, …, P7) (Fig. 3a), and with four skin–markers glued on the anterior aspect of the thigh.

The volunteers assumed eight static postures. One was an orthostatic posture (OP). Five were characterized by the right hip assuming different hip flexion–extension and ad–abduction angles, as occurring during the star–arc (SA) movement used to estimate the hip joint centre (Camomilla et al. 2006, Fig. 2). Two postures regarded walking. The volunteers were asked to mimic the postures as at the beginning (MS1) and at the end (MS2) of the mid–stance phase during which the hip joint under analysis assumes maximal flexion and maximal extension, respectively. To grant stability throughout all of these acquisitions, the volunteers used suitable supports (a stool with adjustable height was used for the SA postures in addition to a

walking frame used for all postures) and were asked to keep the required posture with a moderate and constant muscular activation around hip and knee.

Using an eight–camera stereophotogrammetric system (VICON MX, Motion Systems, Oxford, UK, 100 sample/s) and a wand equipped with a cluster of three makers and a sphere on the tip (Cappozzo et al, 1995), the following experiments were carried out. For each volunteer, assuming each of the eight selected postures, the instantaneous position in the global coordinate system (GCS), defined by the stereophotogrammetric system, of the following individual points were sequentially acquired:

- ^{s}ALs: five on the pelvis (Fig. 3a) and two on the thigh (*point acquisitions*);
- unlabelled points (UPs): over the four prominent bony parts of the pelvis where the soft tissue layer exhibited the smallest thickness (Donati et al., 2008; Fig. 3b) (*cloud acquisitions*).

During each acquisition, the instantaneous global position of the skin–markers was also recorded.

2.1. Pelvic and femur ACSs and representation of the ^{s}ALs and HJCs in them

For each volunteer and each posture, the pose in the GCS of the artefact-free pelvic and femur ACSs were determined. The ^{s}ALs and HJCs were thereafter represented in the relevant ACS. This was obtained through the following procedure.

During all postures and for the point acquisitions, using the global positions of the seven pelvic and two thigh markers, the global poses of the technical coordinate systems associated with the pelvis (TCS_p) and with the thigh (TCS_t) were determined through a least–squares approach (Soderkvist and Wedin, 1993).

During all postures and for the cloud data (UPs) acquired using the wand, a different technical coordinate system (TCS_{cp}) was determined for each cloud using the subsets of markers indicated in Figure 3b. This was made necessary by the fact that, while rolling the wand tip over the skin, adjacent markers could move with respect to the underlying bone. Using the data recorded during the relevant point acquisitions, the transformation matrices between the TCS_p, determined using all seven markers, and the TCS_{cp}, determined using the subsets of markers, were calculated (Fig.4, panel b). By applying these transformations, the data of the four clouds (UPs) could be represented in the same TCS_p together with the point acquisition data (Fig. 4, panel c).

At this point, the cloud data and the subject–specific digital bone model could be registered using the UP–CAST approach. This method optimally matches the surfaces determined during the *cloud acquisitions* (UPs, Fig. 3b) with those identified on the subject–specific pelvic model (mUPs, Fig. 1) (Donati et al., 2008). Since the mUPs are represented in the pelvic ACS and the UPs in the pelvic TCS_P, the mUPs–UPs matching provides the transformation from the TCS_p to the pelvic ACS (Fig.4, panels a and c). Therefore, in each specific acquisition, the pelvic ^sALs, given in the TCS_p, and the HJCs, given in the digital model technical coordinate system, may be represented in the pelvic ACS. It should be emphasised that, using the UP–CAST method, the intra-operator variability of the pelvic ACS orientation, can be kept lower than 0.3 deg, as shown in Donati et al. (2008).

For the thigh, during the relevant *point acquisitions*, the position of the thigh ^sALs was determined in the GCS and subsequently represented in TCS_t. Using the available transformation matrices, the HJCs associated with the pelvic ACS were represented in the thigh TCS_t. Using the positions of the RHJC and of those of ^sRME and ^sRLE, the right femur ACS was obtained according to the definition given in Cappozzo et al. (1995).

2.2. Postures description

Given the pose in the GCS of the pelvic and femur ACSs, obtained as illustrated above, the pelvic ACS orientation, relative to that assumed during the orthostatic posture, and the hip joint angles during each selected posture were assessed. Hip joint angles were determined consistently with the Cardan convention (Wu et al., 2000). Pelvis orientation was computed using the Cardan angular convention and the sequence tilt, obliquity, and rotation.

2.3. STA characterization

To describe the STA affecting a given ^sAL, while assuming an MS or SA posture, we computed the difference between its position vector in the pelvic ACS as observed during the selected posture and during the orthostatic posture (STA vector). In particular, the following parameters were used: for each posture, the amplitude of the STA vector, and, for the ensemble of the two MS and of the SA postures, the distance between the positions of the ^sALs which were farthest away from each other was computed (STA diameter, as defined in Grimpampi et al., 2014).

2.4. Impact of the STA on the estimation of pelvic orientation

The impact of the STA on the estimation of the pelvic orientation for the MS and the SA postures was assessed. For each of these postures, we estimated the orientation of the pelvic

ACS, obtained using the [s]ALs, relative the artefact-free pelvic ACS. Using this orientation matrix, the pelvic orientation error due to STA was quantified in terms of tilt, obliquity, and rotation angles and orientation vector.

Using the same approach, for OP this orientation matrix was computed to assess the unavoidable discrepancies between the manual palpation of the pelvic ALs on the skin and the digital virtual palpation of the same ALs performed on the subject-specific digital bone model.

To put into context the pelvic orientation errors, information on relevant thigh orientation errors is of interest. Given the absence in the literature of such information for the SA postures under analysis, thigh errors were estimated using a model of the STA orientation error as driven by joint kinematics (Camomilla et al. 2013). The model, calibrated in the cited study for the star-arc movement (parameters from subj4), was fed with the subject-specific hip joint angles assumed in this study for the different SA postures (Table 2).

2.5. Statistical analysis

Descriptive statistics of pelvic orientation and hip angles during the analysed postures was carried out, after testing for normal distribution using the normality test Shapiro–Wilk, using the five–number summary technique (box–plots: minimum, lower quartile, median, upper quartile, and maximum).

Differences among [s]ALs and due to the specific group of postures (MS or SA), as well as differences due to BMI (separating normal and overweight volunteers using 25 as threshold) were highlighted. STA amplitudes and diameters were grouped according to [s]ALs, group of postures, and BMI, and a five-number summary descriptive statistics was used for each data group, after testing for normal distribution (Shapiro–Wilk test).

To highlight the inter–subject repeatability of the orientation of the STA vectors, for both the MS and SA postures, these vectors were also averaged over all volunteers and represented in the frontal and sagittal plane.

RESULTS

The characteristics of the static positions assumed by the volunteers are reported in Table 2.

For each volunteer and [s]AL, the STA amplitudes and the STA diameters are reported for the MS and SA postures (Table 3). For the anterior pelvic ALs, the STA amplitudes ranged from 3.1 to 25.4 mm and from 4.6 to 52.1 mm, for normal and overweight volunteers, respectively; for the posterior ALs, from 1.9 to 22.0 mm and from 7.2 to 29.4 mm, for normal and

overweight volunteers, respectively. The ˢRASIS amplitude (median [inter-quartile] value: 16.1 [13.1] mm) was higher than the ˢLASIS amplitude (13.3 [11.1] mm) and the amplitude of all posterior ALs (9.5 [6.1] mm). Similar behaviour was observed for the STA diameters, which were larger for the anterior ALs as compared with the posterior ALs for both MS (7.6 [5.6] vs 3.1 [3.7] mm) and SA postures (14.8 [9.7] vs 10.2 [7.9] mm).

The impact of the amount of soft tissue on STA amplitude can be inferred from Figure 5, where the amplitudes for the different ˢALs are grouped according to BMI. All ˢALs had wider STA amplitudes for the overweight volunteers.

A description of the spatial orientation of the STA vectors for MS and SA postures is provided in Figure 6, where the STA vectors of each ˢAL, averaged over all volunteers, are depicted in the frontal and sagittal plane.

The STA vector impact on pelvis tilt, obliquity, and rotation is reported in Table 4 for MS and SA postures and subjects. The median (inter–quartile) amplitude of the orientation vector was 6.8 (3.9) and 5.8 (3.7) deg, for the two tasks, respectively. The measured pelvic orientation error had half the amplitude of the estimated thigh orientation error (pelvic/femur error median ratio: 0.6; inter–quartile range: 0.5–1.4), over all SA postures.

The pelvic rotations describing the discrepancy between the manual palpation over the skin and virtual palpation of digital bone ALs, were -2.9±1.5, 0.2±3.0, -2.7±1.8 deg, for tilt, obliquity, and rotation, respectively.

DISCUSSION

In this study a multiple anatomical calibration based on a non–invasive and highly repeatable approach was performed and pelvic STA was assessed relative to static postures assumed to resemble the mid–stance phase of gait (MS) and the star–arc movement (SA), entailing hip flexion/extension and ad–abduction ranges of motion larger than during gait. The STA was characterized in terms of amplitude and direction with respect to different ALs, task performed, and subjects' BMI. Pelvic tilt, obliquity, and rotation inaccuracy caused by the STA were in general one order of magnitude larger than the variability of the anatomical calibration procedure used in this study (Donati et al., 2008), confirming the adequateness of the methodological approach.

The STA amplitudes were similar for the two tasks (median 11.1 [12.4] mm, for MS postures, and 11.9 [9.0] mm, for the SA postures) with consequent similar median error in pelvic pose (median orientation vector amplitude, 6.8 [3.9] and 5.8 [3.7] deg, for the two groups of

postures, respectively). Conversely, STA diameters were larger for SA postures than for MS postures, due to the wider range of motion explored within the task. Landmarks displacement was, in general, towards the superior direction for both tasks. The anterior superior spine on the side of the lower limb under analysis, which presented the widest STA, had also a lateral displacement in both tasks, while the contralateral anterior superior spine slightly moved posteriorly. The amplitudes assessed in this study for volunteers with similar BMIs were wider than those presented by Hara at al., 2014, for similar static postures with the hip moved in the sagittal plane (Hara et al., 2014) and smaller than those presented by Rozumalski et al. 2008 for dynamic gait trials. The difference with the former study can be possibly due to the method used for the anatomical calibration and to differences in the hip angular positions, while the differences with the latter study are presumably due to the dynamic conditions. Nevertheless, the general STA behaviour, such as the prevalence of the displacement of the anterior superior spines with respect to the posterior ones and the tendency towards upward marker displacements, were confirmed.

As expected, bigger soft tissues masses, testified by BMI information, were paralleled by an increased STA amplitude for all pelvic areas, being prevalent for the anterior superior iliac spines. The STA amplitude ranges from 2 to 25 mm, for normal weight volunteers, and from 5 to 50 mm, for overweight volunteers. Consequent errors in pelvic pose, measured as amplitude of the relevant orientation vector, ranged from 1 to 9 degrees and from 4 to 11 degrees, for the two groups respectively. These preliminary results, obtained on only two male volunteers, do not allow for any generalization of the results, also in the light of gender–related anthropomorphic differences of the pelvis. They, however, constitute further food for thought in relation to the appropriateness of using marker–based human movement analysis to track the pelvis in overweight subjects (Borhani et al., 2013).

The following major limitations warrant acknowledgment prior to plausibly translating present static results to a dynamic context: (a) the practical complexities intrinsic in having subject–specific bone models limited the sample to five volunteers; (b) skin stretching is the only STA component accounted for due to the lack of muscular activity and inertial effects, normally associated with voluntary *in-vivo* motions. It is, however, important to note that, during functional movements performed in–vivo for HJC determination, the frontal thigh muscles are continuously contracted, the adductors have a minor role, and abduction is mostly performed by the muscles of the gluteal region. This entails that during movement, the soft

tissue deformation due to muscle activation-deactivation and the inertial effects due to impacts or abrupt accelerations are limited.

The detrimental role of STA in the HJC position estimate using the functional approach, often performed using the star–arc movement, has been well documented (Fiorentino et al., 2016), but algorithms that aim at STA compensation accounted only for the thigh STA (De Rosario et al., 2013; Rouhandeh et al., 2014b). Current results call for an expansion to the pelvic segment STA in developing these algorithms.

Conflict of interest statement

The authors do not have any financial or personal relationships with other people or organizations that could inappropriately influence the manuscript.

References

Akbarshahi, M., Schache, A.G., Fernandez, J.W., Baker, R., Banks, S., Pandy, M.G., 2010. Non invasive assessment of soft-tissue artifact and its effect on knee joint kinematics during functional activity. Journal of Biomechanics 43(7), 1292–301.

Andersen, M.S., Damsgaard, M., Rasmussen, J., Ramsey, D.K., Benoit, D.L., 2012. A linear soft tissue artefact model for human movement analysis: proof of concept using in vivo data. Gait & Posture 35(4), 606–11.

Benoit, D.L., Ramsey, D.K., Lamontagne, M., Xu, L., Wretenberg, P., Renström, P., 2006. Effect of skin movement artifact on knee kinematics during gait and cutting motions measured in vivo. Gait & Posture 24(2), 152–164.

Bonci, T., Camomilla, V., Dumas, R., Chèze, L., Cappozzo, A., 2014. A soft tissue artefact model driven by proximal and distal joint kinematics. Journal of Biomechanics 47(10), 2354–2361.

Borhani, M., McGregor, A.H., Bull, A.M.J., 2013. An alternative technical marker set for the pelvis is more repeatable than the standard pelvic marker set. Gait & Posture 38 (4), 1032–1037.

Camomilla, V., Cereatti, A., Chèze, L., Cappozzo, A., 2013. A hip joint kinematics driven model for the generation of realistic thigh soft tissue artefacts. Journal of Biomechanics 46 (3), 625-630.

Camomilla, V., Cereatti, A., Vannozzi, G., Cappozzo, A., 2006. An optimized protocol for hip joint centre determination using the functional method. Journal of Biomechanics 39 (6), 1096–1106.

Cappozzo, A., Catani, F., Della Croce, U., Leardini, A., 1995. Position and orientation of bones during movement: anatomical frame definition and determination. Clinical Biomechanics 10 (4), 171–178.

Cappozzo, A., Catani, F., Leardini, A., Benedetti, M.G., Della Croce, U., 1996. Position and orientation in space of bones during movement: experimental artefacts. Clinical Biomechanics 11 (2), 90-100.

Cappozzo, A., Cappello, A., Della Croce, U., Pensalfini, F., 1997. Surface–Marker Cluster Design Criteria for 3–D Bone Movement Reconstruction. IEEE Transactions on Biomedical Engineering 44 (12), 1165–1174.

Cappozzo, A., Della Croce, U., Leardini, A., Chiari, L., 2005. Human movement analysis using stereophotogrammetry. Part1: theoretical background. Gait & Posture 21 (2), 186–196.

Cereatti, A., Donati, M., Camomilla, V., Margheritini, F., Cappozzo, A., 2009. Hip joint centre location: an ex vivo study. Journal of Biomechanics 42(7), 818–823.

Charbonnier, C., Chague, S., Kolo, F. C., Chow, J. C. K., Lädermann, A., 2014. A patient-specific measurement technique to model shoulder joint kinematics. Orthopaedics & Traumatology: Surgery & Research 100(7), 715–719.

Dal Maso, F., Blache, Y., Raison, M., Lundberg, A., Begon, M., 2016. Glenohumeral joint kinematics measured by intracortical pins, reflective markers, and computed tomography: A novel technique to assess acromiohumeral distance. Journal of Electromyography and Kinesiology 29, 4 – 11.

De Rosario, H., Page, Á., Besa, A., Valera, Á., 2013. Propagation of soft tissue artifacts to the center of rotation: A model for the correction of functional calibration techniques. Journal of Biomechanics 46 (15), 2619–2625.

Donati, M., Camomilla, V., Vannozzi, G., Cappozzo, A. 2008. Anatomical frame identification and reconstruction for repeatable lower limb joint kinematics estimates. Journal of Biomechanics 41 (10), 2219–2226.

Donati, M., Camomilla, V., Vannozzi, G., Cappozzo, A., 2007. Enhanced anatomical calibration in human movement analysis. Gait & Posture 26 (2), 179–185.

Fiorentino, N.M., Atkins, P.R., Kutschke, M.J., Foreman, K.B., Anderson, A.E., 2016. In-vivo quantification of dynamic hip joint center errors and soft tissue artifact. Gait & Posture. 50, 246-251.

Fuller, J., Liu, L., Murphy, M., Mann, R., 1997. A comparison of lower-extremity skeletal kinematics measured using skin-and pin-mounted markers. Human Movement Science 16(2), 219–242.

Grimpampi, E., Camomilla, V., Cereatti, A., De Leva, P., Cappozzo, A., 2014. Metrics for describing soft-tissue artefact and its effect on pose, size, and shape of marker clusters. IEEE Transactions on Biomedical Engineering 61 (2), 362-367.

Hara, R., Sangeux, M., Baker, R., & McGinley, J., 2014. Quantification of pelvic soft tissue artifact in multiple static positions. Gait & Posture 39 (2), 712–717.

Holden, J.P., Orsini, J.A., Siegel, K.L., Kepple, T.M., Gerber, L.H., Stanhope, S.J., 1997. Surface movement errors in shank kinematics and knee kinetics during gait. Gait & Posture 5 (3), 217-227.

Houck, J., Yack, H.J., Cuddeford, T., 2004. Validity and comparisons of tibiofemoral orientations and displacement using a femoral tracking device during early to mid stance of walking. Gait & Posture 19(1), 76–84.

Kainz, H., Carty, C.P., Modenese, L., Boyd, R.N., Lloyd, D.G., 2015. Estimation of the hip joint centre in human motion analysis: a systematic review. Clinical Biomechanics 30 (4), 319-29.

Kuo, M.-Y., Tsai, T.-Y., Lin, C.-C., Lu, T.-W., Hsu, H.-C., Shen, W.-C., 2011. Influence of soft tissue artifacts on the calculated kinematics and kinetics of total knee replacements during sit to-stand. Gait & Posture 33(3), 379–84.

Lafortune, M.A., Cavanagh, P.R., Sommer, H.J., Kalenak, A., 1992. Three-dimensional kinematics of the human knee during walking. Journal of Biomechanics 25(4), 347–357.

Leardini, A., Chiari, L., Della Croce, U., Cappozzo, A., 2005. Human movement analysis using stereophotogrammetry. Part 3. Soft tissue artifact assessment and compensation. Gait & Posture 21(2), 212-25.

Manal, K., McClay, I., Stanhope S.J., Richards, J., Galinat, B., 2000. Comparison of surface mounted markers and attachment methods in estimating tibial rotations during walking: an in vivo study. Gait & Posture 11(1), 38 – 45.

Maslen, B., Ackland, T.R., 1994. Radiographic study of skin displacement errors in the foot and ankle during standing. Clinical Biomechanics 9(5), 291–296.

Peters, A., Galna, B., Sangeux, M., Morris, M., Baker, R., 2010. Quantification of soft tissue artifact in lower limb human motion analysis: a systematic review. Gait & Posture 31 (1), 1-8.

Ramsey, D.K., Wretenberg, P.F., Benoit, D.L., Lamontagne, M., Németh, G., 2003. Methodological concerns using intra-cortical pins to measure tibiofemoral kinematics. Knee Surgery, Sports Traumatology, Arthroscopy 11(5), 344–349.

Reinschmidt, C., Van Den Bogert, A.J., Nigg, B.M., Lundberg, A., Murphy, N., 1997. Effect of skin movement on the analysis of skeletal knee joint motion during running. Journal of Biomechanics 30(7), 729–732.

Rouhandeh, A., Joslin, C., Zhen, Qu, Yuu, Ono, 2014a. Non-invasive assessment of soft-tissue artefacts in hip joint kinematics using motion capture data and ultrasound depth measurements. IEEE Engineering in Medicine and Biology Society Annual Conference. 2014, 4342-5.

Rouhandeh, A., Joslin, C., Zhen, Qu, Yuu, Ono, 2014b. Soft-tissue artefact assessment and compensation in hip joint kinematics using motion capture data and ultrasound depth measurements. International Conference on Biomedical Engineering and Systems, Prague, 2014.

Rozumalski, A., Schwartz, M., Novacheck, T., Wervey, R., Swanson, A., Dykes, D., 2007. Quantification of pelvic soft tissue artifact. Gait Clin. Mov. Anal. Soc., 10–11.

Sati, M., De Guise, J., Larouche, S., Drouin, G., 1996. Quantitative assessment of skin-bone movement at the knee. The Knee 3(3), 121–138.

Söderkvist, I., Wedin, P.A., 1993. Determining the movements of the skeleton using well–configured markers. Journal of Biomechanics 26 (12), 1473–1477.

Stagni, R., Leardini, A., Cappozzo, A., Benedetti, M.G., Cappello, A., 2000. Effects of hip joint centre mislocation on gait analysis results. Journal of Biomechanics 33(11), 1479-87.

Stagni, R., Fantozzi, S., Cappello, A., Leardini, A., 2005. Quantification of soft tissue artefact in motion analysis by combining 3D fluoroscopy and stereophotogrammetry: a study on two subjects. Clinical Biomechanics 20(3), 320–329.

Stalling, D., Westerhoff, M., Hege, H.-C. 2005. C.D. Hansen and C.R. Johnson, ed. "Amira: A Highly Interactive System for Visual Data Analysis". The Visualization Handbook. Elsevier: 749–767. CiteSeerX 10.1.1.129.6785

Tsai, T.-Y., Lu, T.-W., Kuo, M.-Y., Hsu, H.-C., 2009. Quantification of Three-Dimensional Movement of Skin Markers Relative To the Underlying Bones During Functional Activities. Biomedical Engineering: Applications, Basis and Communications 21(03), 223–232.

Tsai, T.-Y., Lu, T.-W., Kuo, M.-Y., Lin, C.-C., 2011. Effects of soft tissue artifacts on the calculated kinematics and kinetics of the knee during stair-ascent. Journal of Biomechanics 44(6), 1182–1188.

Van Sint Jan, S., 2007. Color atlas of skeletal landmark definitions. Guidelines for Reproducible Manual and Virtual Palpations. Churchill Livingstone Title.

Westblad, P., Hashimoto, T., Winson, I., Lundberg, A., Arndt, A., 2002. Differences in ankle-joint complex motion during the stance phase of walking as measured by superficial and bone-anchored markers. Foot & Ankle International 23(9), 856-63.

Wu, G., Siegler, S., Allard, P., Kirtley, C., Leardini, A., Rosenbaum, D., Whittle, M., D'Lima, D.D., Cristofolini, L., Witte, H., Schmid, O., Stokes, I., 2002. ISB recommendation on definitions of joint coordinate system of various joints for the reporting of human joint motion — Part I: ankle, hip, and spine. Journal of Biomechanics 35(4), 543–548.

Figure captions:

Figure 1 Bone digital model of the pelvic skeleton of one volunteer derived from MRI images and carrying the relevant ALs: right and left anterior superior iliac spines – RASIS, LASIS; right and left posterior superior iliac spines – RPSIS, LPSIS; right and left hip joint centres – RHJC, LHJC. The anatomical coordinate system (ACS) and the model unlabelled–points (mUPs) are also shown.
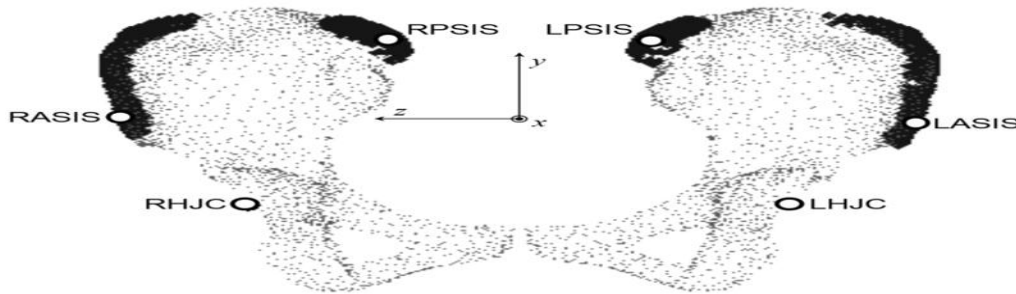
Figure 2 The five different hip positions that characterized the star–arc movement (SA_1, SA_2, SA_3, SA_4, SA_5) are shown in the transverse (a) and frontal plane (b). Numbered segments have lengths that are proportional to the hip angle.

Figure 3 a) Pelvic bone digital model and skin–markers glued on the pelvis (P1, …, P7; grey dots). The position of the ^sALs (^sRASIS, ^sLASIS, ^sRPSIS, ^sLPSIS, ^sSACR) is also shown (black dots) b) Pelvic bone digital model and UPs acquired during the different *cloud acquisitions* (Cloud RASIS, Cloud LASIS, Cloud RPSIS, Cloud LPSIS). The skin–markers used to construct the technical coordinate system with respect to which each *cloud acquisition* is represented, TCS_{cp}, are also reported (grey markers).

Figure 4 Dark grey boxes contain the pose of the indicated technical coordinate system with respect to the global coordinate system; light grey boxes contain points represented in the specified coordinate system, white boxes contain coordinate system registration matrices. Uppe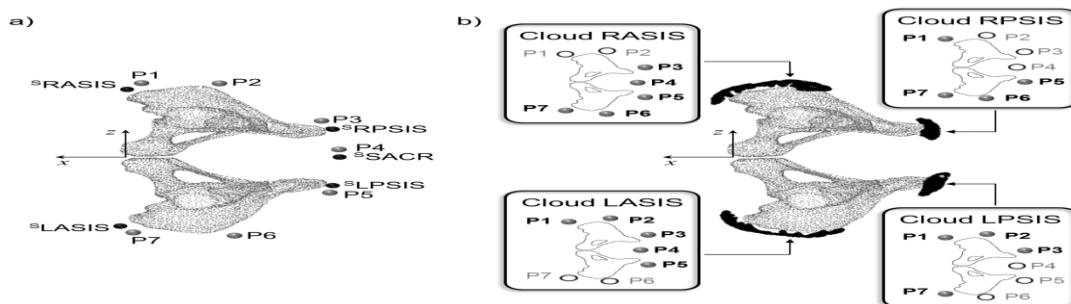r box: for each volunteer **a)** representation of mUPs in the pelvic anatomical coordinate system, ACS, defined on the subject–specific bone template. Lower box: for each posture, **b)** registration between the pelvic technical coordinate system obtained using all available pelvis markers, TCS_p, and each cloud–specific technical coordinate system obtained using markers depicted in Fig. 2a, TCS_{cp}; **c)** representation of the UPs acquired during the cloud acquisitions in the TCS_p using the registration matrix produced in phase b; **d)** representation of the ^sALs in the TCS_p. Thereafter, for each posture, the mUPs and UPs information obtained in panels a and c are used to obtain the registration between ACS and TCS_p which, in turn, is used to finally represent each ^sAL in the pelvic ACS.
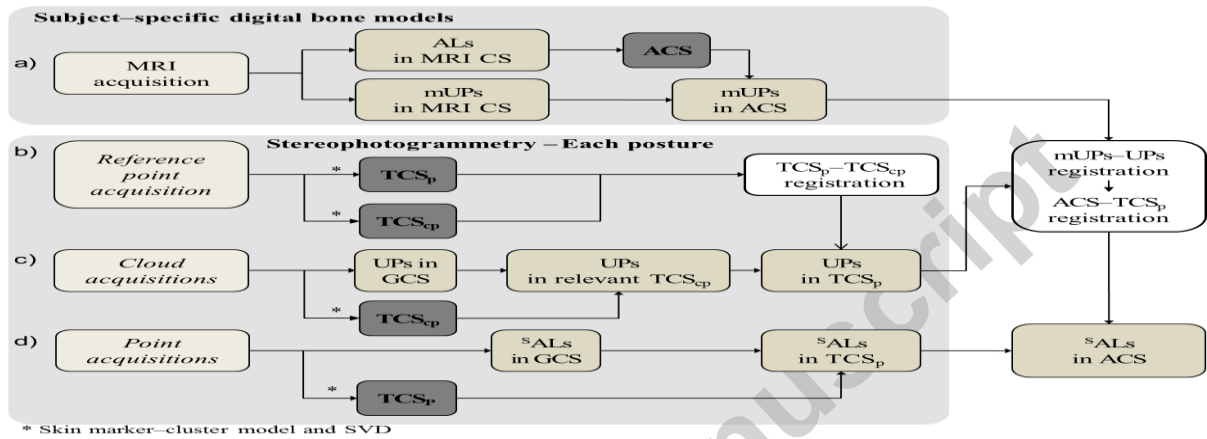

Figure 5 Box–plots (minimum, lower quartile, median, upper quartile, and maximum) of the STA amplitudes measured in all the analysed postures for the different ^sALs (^sLASIS, ^sRASIS, ^sLPSIS, ^sRPSIS, and ^sSACR). Outliers are also depicted. These values are presented for normal–weight (BMI<25) and overweight volunteers (BMI≥25), in white and grey, respectively.
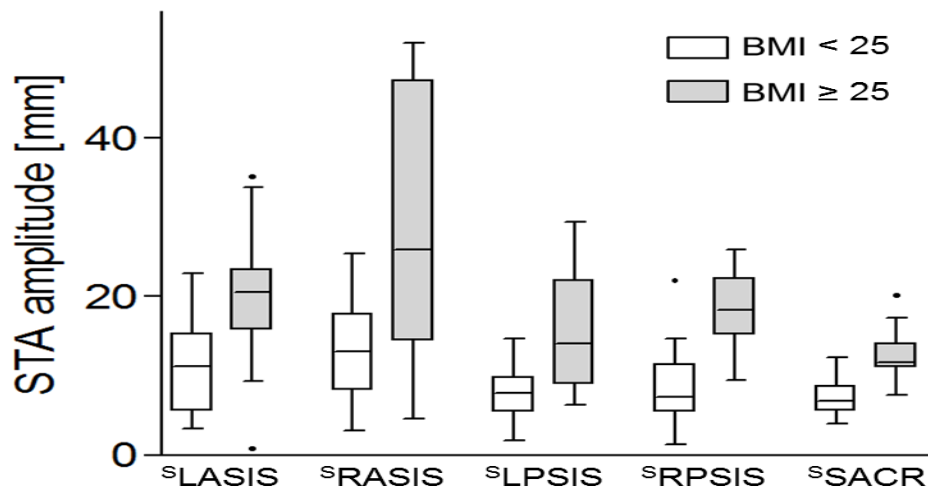
Figure 6 Mean STA vectors for the different ^{s}ALs (^{s}LASIS, ^{s}RASIS, ^{s}LPSIS, ^{s}RPSIS, ^{s}SACR), averaged over all volunteers, separately for mid–stance (on the left) and star–arc postures (on the right). Upper panel: vectors projection on the frontal plane. Lower panel: vectors projection on the sagittal plane.
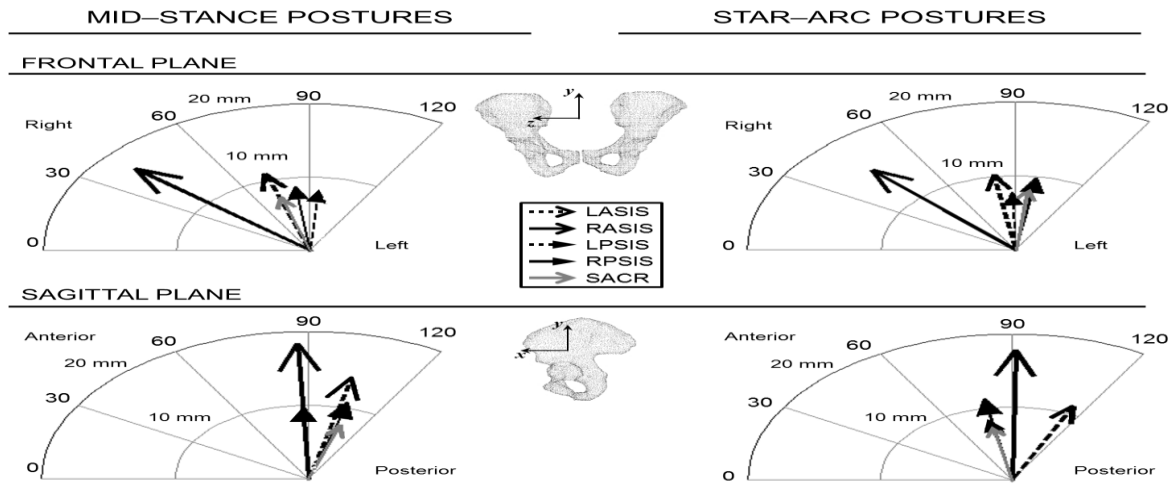

Table 1 Age, gender, and anthropometric profile of the volunteers (V1…V5) involved in the study.

	V1	V2	V3	V4	V5
Height [cm]	164	161	194	171	178
Mass [kg]	60	60	90	83	117
BMI [kg/m^2]	22.3	23.1	23.9	28.4	36.9
Gender	F	F	M	M	M
Age [y]	42	47	37	44	48

Table 2 Lower quartile (1st), median and upper quartile (3rd) of the angles (FE, hip flexion–extension; AA, hip ab–adduction; IE, internal-external rotation: pelvic tilt, and pelvic obliquity) measured in orthostatic posture (OP), in the two gait mid–stance postures grouped as if it were one (MS), and in the five static postures of the star–arc movement (SA1,…, SA5). Pelvis orientation was obtained with respect to the global coordinate system, for OP, and with respect to OP orientation, for the others postures. Pelvic rotation in the transverse plane were not reported since they are related to experimental requirements and not to the motor task performed.

	Angle	OP	MS	SA1	SA2	SA3	SA4	SA5
FE	1st quartile	2.1	5.3	49.6	28.4	17.0	-8.7	-15.5
	median	4.7	15.9	49.7	45.2	17.5	-2.2	-6.5
	3rd quartile	6.4	25.3	57.0	45.5	29.1	3.5	-6.4
AA	1st quartile	0.7	-2.7	11.4	29.8	36.6	26.5	14.9
	median	3.2	0.9	17.0	37.5	41.7	29.6	17.9
	3rd quartile	9.7	9.9	17.8	43.4	54.4	30.0	22.4
IE	1st quartile	4.8	-2.0	17.1	8.4	4.9	-16.4	-5.7
	median	7.5	7.0	32.6	35.4	5.5	1.6	1.9
	3rd quartile	8.2	16.1	41.2	42.4	8.5	29.7	2.5
pelvic obliquity	1st quartile	2.1	-3.3	-2.0	-0.9	1.5	2.1	0.9
	median	2.3	0.5	0.5	2.4	5.2	3.2	1.7

	3rd quartile	4.1	2.2	3.3	7.8	5.3	4.3	2.1
pelvic tilt	*1st quartile*	4.4	3.6	-2.0	-1.7	2.7	8.6	9.3
	median	6.3	5.5	3.2	0.3	3.7	8.7	10.9
	3rd quartile	6.7	6.4	3.4	0.8	3.8	13.8	12.6

Table 3 STA amplitude values in mm measured for each volunteer (V1, ..., V5), ^{s}AL and the MS postures, grouped as if it were one, and all SA postures (SA1, …, SA5). STA diameter values, relative to the postures assumed during gait mid–stance (MS) and star–arc (SA) tasks, are also shown. BMI information is reported in kg/m^2.

			STA amplitude						STA diameter	
		BMI	MS	SA1	SA2	SA3	SA4	SA5	MS	SA
LASIS	V1	*22.3*	18.8	11.2	11.3	5.4	16.3	11.9	8.2	10.9
	V2	*23.1*	9.3	3.3	5.0	6.4	10.3	5.9	7.0	7.0
	V3	*23.9*	10.8	15.4	15.3	8.8	3.5	15.7	13.6	12.2
	V4	*28.4*	8.5	9.3	23.4	20.7	20.9	33.8	15.4	24.5
	V5	*36.9*	29.3	20.3	19.1	14.7	20.5	23.3	11.6	8.6
RASIS	V1	*22.3*	11.5	16.5	12.9	8.2	18.7	9.7	2.4	10.6
	V2	*23.1*	10.6	15.6	6.2	25.4	13.3	7.0	4.9	19.2
	V3	*23.9*	11.5	17.8	23.9	19.3	3.1	17.7	11.3	20.8
	V4	*28.4*	24.5	4.6	14.5	14.0	11.1	22.0	6.2	17.4
	V5	*36.9*	44.9	50.3	52.1	24.4	47.2	35.2	5.8	27.7
LPSIS	V1	*22.3*	7.8	7.1	1.9	10.4	12.1	6.3	1.6	10.2
	V2	*23.1*	7.1	14.6	8.4	4.7	4.2	11.6	1.5	10.4
	V3	*23.9*	5.5	11.0	9.0	4.6	7.9	9.2	3.1	6.4
	V4	*28.4*	14.8	7.5	11.1	11.3	21.6	29.4	17.0	21.9
	V5	*36.9*	20.1	9.4	19.3	18.1	13.1	7.2	9.8	12.1
RPSIS	V1	*22.3*	9.4	5.7	7.3	8.1	10.3	5.6	5.1	4.7
	V2	*23.1*	4.6	4.1	5.2	22.0	9.3	11.6	1.4	17.9
	V3	*23.9*	3.9	14.7	11.2	6.9	12.9	8.4	5.1	7.8
	V4	*28.4*	20.1	15.6	11.3	14.7	25.9	15.4	2.6	14.5
	V5	*36.9*	22.5	16.6	24.7	17.8	20.7	9.5	6.5	15.3
SACR	V1	*22.3*	6.9	9.0	5.1	6.8	5.0	3.9	0.3	5.1
	V2	*23.1*	6.8	8.1	9.6	8.6	6.2	12.3	0.3	6.1
	V3	*23.9*	5.5	10.9	5.9	5.7	9.0	7.4	0.1	5.2
	V4	*28.4*	11.8	13.0	11.4	8.2	11.5	11.6	3.3	4.8
	V5	*36.9*	15.8	11.4	20.2	14.1	11.9	7.7	3.1	12.5

Table 4 The pelvic orientation error in degrees measured for each volunteer (V1, ..., V5) for the MS postures, grouped as if it were one, and all SA postures (SA1, …, SA5).

		MS	SA1	SA2	SA3	SA4	SA5
Pelvic tilt	V1	4.5	2.7	2.2	4.3	5.1	4.6
	V2	-0.1	1.4	0.0	-1.4	-0.9	-3.0
	V3	3.0	-1.1	5.6	2.7	-2.3	4.0
	V4	4.8	3.3	-0.3	2.0	6.0	-1.3
	V5	3.4	7.5	4.5	4.3	4.3	-0.1
Pelvic obliquity	V1	-4.4	1.9	1.6	1.8	-0.2	-0.7
	V2	3.5	2.7	1.6	8.1	4.0	1.3
	V3	0.2	3.6	1.2	2.2	-0.1	0.5
	V4	-2.8	-2.0	-0.7	-1.4	-2.1	-5.8
	V5	6.4	5.4	6.6	3.3	4.8	4.8
Pelvic rotation	V1	2.2	2.7	2.7	0.2	-1.7	1.3
	V2	0.8	0.8	0.4	-0.4	2.4	-0.8
	V3	1.2	2.5	0.2	0.3	0.6	-2.2
	V4	4.3	-1.6	6.1	6.0	5.5	8.5
	V5	-4.0	-4.8	-7.5	-0.2	-7.7	-5.8